BBA - Molecular Basis of Disease 1865 (2019) 2210–2223

Contents lists available at ScienceDirect

BBA - Molecular Basis of Disease

journal homepage: www.elsevier.com/locate/bbadis

COL1A1 C-propeptide mutations cause ER mislocalization of procollagen and impair C-terminal procollagen processing

Aileen M. Barnes[a], Aarthi Ashok[a,b,1], Elena N. Makareeva[c], Marina Brusel[d], Wayne A. Cabral[a,e,1], MaryAnn Weis[f], Catherine Moali[g], Emmanuel Bettler[g], David R. Eyre[f], John P. Cassella[h], Sergey Leikin[c], David J.S. Hulmes[g], Efrat Kessler[d], Joan C. Marini[a,*]

[a] Section of Heritable Disorders of Bone and Extracellular Matrix, NICHD, NIH, Bethesda, MD, United States of America
[b] University of Toronto Scarborough, Toronto, ON, Canada
[c] Section on Physical Biochemistry, NICHD, NIH, Bethesda, MD, United States of America
[d] Goldschleger Eye Research Institute, Tel Aviv University Sackler Faculty of Medicine, Tel-Hashomer, Israel
[e] Molecular Genetics Section, Medical Genomics and Metabolic Genetics Branch, NHGRI, NIH, Bethesda, MD, United States of America
[f] Orthopaedic Research Labs, University of Washington, Seattle, WA, United States of America
[g] Tissue Biology and Therapeutic Engineering Unit, UMR5305, CNRS/University of Lyon, Lyon, France
[h] Department of Forensic and Crime Science, Staffordshire University, Staffordshire, UK

ARTICLE INFO

Keywords:
Osteogenesis imperfecta
Collagen processing
C-propeptide
BMP-1
Endoplasmic reticulum localization

ABSTRACT

Mutations in the type I procollagen C-propeptide occur in ~6.5% of Osteogenesis Imperfecta (OI) patients. They are of special interest because this region of procollagen is involved in α chain selection and folding, but is processed prior to fibril assembly and is absent in mature collagen fibrils in tissue. We investigated the consequences of seven *COL1A1* C-propeptide mutations for collagen biochemistry in comparison to three probands with classical glycine substitutions in the collagen helix near the C-propeptide and a normal control. Procollagens with C-propeptide defects showed the expected delayed chain incorporation, slow folding and overmodification. Immunofluorescence microscopy indicated that procollagen with C-propeptide defects was mislocalized to the ER lumen, in contrast to the ER membrane localization of normal procollagen and procollagen with helical substitutions. Notably, pericellular processing of procollagen with C-propeptide mutations was defective, with accumulation of pC-collagen and/or reduced production of mature collagen. *In vitro* cleavage assays with BMP-1 ± PCPE-1 confirmed impaired C-propeptide processing of procollagens containing mutant proα1(I) chains. Overmodified collagens were incorporated into the matrix in culture. Dermal fibrils showed alterations in average diameter and diameter variability and bone fibrils were disorganized. Altered ER-localization and reduced pericellular processing of defective C-propeptides are expected to contribute to abnormal osteoblast differentiation and matrix function, respectively.

1. Introduction

Osteogenesis Imperfecta (OI), also known as brittle bone disease, is mainly caused by dominantly inherited mutations in *COL1A1* or *COL1A2* that alter the structure or decrease the production of type I collagen. The Sillence classification divides OI caused by collagen defects into four types, including mild type I, caused by a null *COL1A1* allele, moderately severe type IV, progressive deforming type III, and

Abbreviations: BSA, bovine serum albumin; BMP-1, bone morphogenetic protein-1; BTPs, BMP-1/tolloid-like proteinases; CPI, C-propeptide of type I collagen; CPIII, C-propeptide of type III collagen; DMEM, Dulbecco's modified Eagle medium; DSC, differential scanning calorimetry; EDS, Ehlers-Danlos syndrome; EDTA, ethylenediaminetetraacetic acid; ER, endoplasmic reticulum; FBS, fetal bovine serum; gDNA, genomic deoxyribonucleic acid; IRB, institutional review board; NICHD, the *Eunice Kennedy Shriver* National Institute of Child Health and Human Development; NIH, National Institutes of Health; OI, osteogenesis imperfecta; PAGE, polyacrylamide gel electrophoresis; PBS, phosphate buffered saline; PCPE-1, procollagen C-proteinase enhancer-1; PCR, polymerase chain reaction; PMSF, phenylmethylsulfonyl fluoride; rER, rough endoplasmic reticulum; SDS, sodium dodecyl sulfate

* Corresponding author at: Section on Heritable Disorders of Bone and Extracellular Matrix, NICHD, NIH, Bldg. 49; Rm 5A52, 9000 Rockville Pike, Bethesda, MD 20892, United States of America.
E-mail address: oidoc@helix.nih.gov (J.C. Marini).
[1] Current address.

https://doi.org/10.1016/j.bbadis.2019.04.018
Received 10 December 2018; Received in revised form 15 April 2019; Accepted 30 April 2019
Available online 02 May 2019

perinatal lethal type II [1]. Types II-III-IV OI are caused by structural defects in either collagen chain, most commonly substitutions of one of the invariant glycine residues (Gly-Xaa-Yaa) that are critical for tight helical folding. Clinical features of OI caused by collagen structural defects include increased fracture susceptibility, bowing of the long bones, macrocephaly, blue sclerae, dentinogenesis imperfecta, hearing loss, scoliosis and pectal deformity [2].

Type I collagen is the major protein component of the extracellular matrix of bone and skin. Type I collagen is a heterotrimeric fibrillar collagen, containing two α1 and one α2 chains. In the cell, type I collagen is synthesized as procollagen, with amino (N-) and carboxyl (C-) terminal propeptides flanking the central triple helical region. The C-propeptide of type I collagen is critical for both chain alignment and recognition during procollagen synthesis, to obtain the proper 2:1 chain composition [3–5]. Unlike the type I collagen helix, the C-propeptide contains critical cysteine residues that participate in both intra- and inter-chain disulfide bonds. Stabilization of the C-propeptide creates a nucleation site to initiate folding, which then proceeds in a zipper-like fashion from the C– to the N-terminus [6]. Procollagen is subsequently secreted into the pericellular space, where the terminal propeptides are cleaved by specific procollagen N- and C-proteinases. Finally, the mature collagen molecules aggregate spontaneously into fibrils.

The C-propeptide is processed by members of the bone morphogenetic protein-1 (BMP-1)/tolloid-like proteinases (BTPs) family [7–9], of which BMP-1 is probably the most active and best characterized. BTP activity towards procollagens I-III is increased specifically by an extracellular matrix glycoprotein called procollagen C-proteinase enhancer 1 (PCPE-1) [10–12].

Mutations affecting conserved residues in the type I procollagen C-propeptide have been shown to cause ~ 6.5% of OI cases [13]. Since the C-propeptide is cleaved before mature collagen molecules are incorporated into fibrils, the impact of these defects on bone quality was not anticipated. Crystal structures of the C-propeptide trimers from procollagen III [14] and the homotrimeric form of procollagen I [4] have been determined. While the former (CPIII) provided a useful model to correlate the severity of OI mutations with their positions in the C-propeptide [13], the more recent homo-CPI structure [4] relates directly to procollagen I and is more appropriate for the study of OI-causing mutations.

In this report, we present biochemical investigations on cells from 7 OI probands with *COL1A1* C-propeptide mutations including 6 new cases. We compared the effects of these mutations on collagen folding, ER-localization, procollagen processing and matrix incorporation with three glycine substitutions located near the carboxyl-end of the collagen helix and a normal control. Our fibroblast studies show that procollagens with C-propeptide mutations are mislocalized to the ER lumen and have impaired C-propeptide processing. These studies shed new light on the mechanism of C-propeptide mutations in OI and suggest novel functions for this domain beyond control of collagen trimer assembly.

2. Materials and methods

2.1. Cell culture

Dermal biopsies and osteotomy bone chips were obtained from probands and healthy individuals with informed consent under an NICHD IRB-approved protocol. Fibroblasts were cultured in Dulbecco's Modified Eagle Medium (DMEM, Gibco, Gaithersburg, MD, USA) containing 10% fetal bovine serum (FBS, Gemini Bio-Products, West Sacramento, CA, USA), 2 mM glutamine, 100 Units/ml penicillin and 100 μg/ml streptomycin in the presence of 5% CO_2. Control fibroblasts (ATCC 2127, Manassas, VA, USA) were grown under the same conditions. Osteoblast primary cultures were established as previously described by Robey and Termine [15]. Briefly, osteoblasts were released from bone chips by digestion with Collagenase P (Roche, Basel, Switzerland) at 0.3 U per ml of serum-free medium, for 2 h at 37 °C. Cells were then grown at 37 °C in a 1:1 mixture of low calcium DMEM (Biosource, Camarillo, CA, USA) and low calcium HAMS-F12 medium (Biosource) supplemented with 10% FBS and 25 μg/ml ascorbic acid (Sigma-Aldrich, St. Louis, MO, USA). Only first or second passage osteoblasts were used.

2.2. Mutation detection

Total RNA was harvested from proband and control fibroblasts using Tri Reagent (Molecular Research Center, Cincinnati, OH, USA). The RNA was reverse transcribed using an antisense primer to the 3′-untranslated region of α1(I) collagen (5′-GGAAAGTTGGTTGGGTGGG AGGGAGCCAGG-3′) and used as a template for all overlapping polymerase chain reactions (PCR) to amplify exons 40–52 of *COL1A1* (GenBank RefSeq NM_000088.3, NG_007400.1). RT-PCR products were sequenced directly using a Beckman Coulter CEQ2000 DNA sequencer (Beckman, Fullerton, CA, USA). Confirmation of mutations was done by restriction enzyme digestion of control and proband genomic DNA (gDNA) isolated using the manufacturer's protocol (Gentra Puregene Blood Kit, Qiagen, Hilden, Germany) and then run on agarose or acrylamide gels. The *COL1A1* variants were submitted to the OI variant database (http://lovd.nl/COL1A1).

2.3. Structural analysis of mutations

To analyze the structural consequences of the mutations, the sites of the mutations were identified using the recent crystal structure of the C-propeptide homotrimer (three α1 chains) from human procollagen I (CPI) [4]. We also used a model for the CPI heterotrimer (two α1 chains and one α2 chain) based on the CPI structure and the results of site-directed mutagenesis [4]. This model was built by homology modeling, substituting one of the α1 chains in CPI by an α2 chain then carrying out energy minimization with constraints based on [4] using the program YASARA [16]. Both structures were then analyzed and displayed using Chimera [17]. The coordinates of the CPI heterotrimer model are available on request (to D.J.S.H.).

2.4. Steady-state collagen biochemical analysis

Confluent fibroblast cultures were incubated for 2 h in serum-free DMEM + 50 μg/ml ascorbic acid, then labeled with 260 μCi/ml of 3.96 TBq/mmole L-[2,3,4,5-^{3}H]-proline (Moravek, Brea, CA, USA) in serum-free ascorbate-containing medium for 16 h. Procollagens were harvested from media and cell layer and precipitated with 1/3 volume of saturated ammonium sulfate. Collagens were prepared by pepsin digestion (50 μg/ml) of procollagen samples [18]. Samples were electrophoresed on 6% SDS-urea-PAGE (0.5 M urea).

2.5. Differential scanning calorimetry

Differential scanning calorimetry (DSC) of procollagen and collagen solutions in 0.2 M sodium phosphate and 0.5 M glycerol at pH 7.4 was performed from 10 to 55 °C in a Nano III DSC instrument (Calorimetry Sciences Corporation, Lindon, UT, USA), as previously described [19].

2.6. Mass spectrometry and amino acid analysis

Procollagen prolyl 3-hydroxylation was assessed by ion-trap mass spectrometry, as previously described [20]. Secreted procollagen was precipitated by 1 M $(NH_4)_2SO_4$, from which proα-chains were resolved by SDS-PAGE and subjected to in-gel trypsin digestion for analysis of targeted peptides by electrospray mass spectrometry. Amino acid analysis of hydroxylysine and hydroxyproline content was performed on secreted procollagen by high pressure liquid chromatography on a Hitachi L8900 Amino Acid Analyzer (AAA Service Lab, Damascus, OR, USA).

2.7. Chain association

Confluent fibroblast cultures were incubated for 2 h in serum-free DMEM + 50 μg/ml ascorbic acid, then labeled with 100 μCi/ml of 3.96 TBq/mmole L-[2,3,4,5-^{3}H]-proline in serum-free ascorbate-containing medium for 80 min. The medium was then replaced with DMEM containing 10% FBS, 50 μg/ml ascorbic acid, 2 mM glutamine and 10 mM non-radioactive proline. The cell layer was harvested in PBS containing protease inhibitors (15 mM iodoacetamide, 25.5 mM EDTA, 6.7 μM *N*-ethylmaleimide, 10 μM PMSF and 2.2 nM pepstatin) at 0, 20, 40, 60, 80 and 120 min. Cell procollagens were precipitated with 1/3 volume 100% ethanol plus 19 μg/ml type I calf skin carrier collagen (Sigma-Aldrich). Samples were electrophoresed, under non-reducing conditions, on 5.5% SDS-urea-PAGE (0.5 M urea).

2.8. Folding assay

The intracellular folding assay was performed as described previously [21]. Briefly, confluent fibroblast cultures were labeled with a 15-min ^{14}C-proline pulse, then the cell layer was collected every 5 min. Each sample was collected in PBS containing protease inhibitors plus 0.2% Triton X-100, digested for 2 min with 100 μg/ml trypsin and 250 μg/ml chymotrypsin (Sigma-Aldrich), then stopped with 1 mg/ml soybean trypsin inhibitor (Sigma-Aldrich). Samples were salt precipitated and run on 3–8% Tris-acetate gels (Life Technologies) to distinguish between folded and unfolded collagen chains. Collagen bands were quantitated by densitometry using ImageJ software. The quantity of control cell collagen folded at 30 min was considered to be 100% folded.

2.9. Pericellular processing

Processing of procollagens secreted by fibroblasts was examined by labeling confluent fibroblasts with 260 μCi/ml of 3.96 TBq/mmole L-[2,3,4,5-^{3}H]-proline for 24 h and then chasing with DMEM containing 10% FBS, 2 mM glutamine and 2 mM non-radioactive proline. Media from independent wells was harvested at 24 h intervals over a five-day period (modified from [22]). Media procollagen samples from fibroblasts were precipitated with ammonium sulfate and then electrophoresed on reducing 6% SDS-urea-PAGE (0.5 M urea).

2.10. Matrix deposition

Confluent fibroblasts were stimulated every other day for 9 days with fresh DMEM medium containing 10% FBS, 2 mM glutamine and 100 μg/ml ascorbic acid. Cultures were then incubated for 24 h with 260 μCi/ml of L-[2,3,4,5-^{3}H]-proline in serum-free medium. Medium was collected and procollagens were precipitated with ammonium sulfate. Matrix collagens were serially extracted at 4 °C as previously described [23]. In brief, newly synthesized collagens were extracted for 24 h with neutral salt (50 mM Tris-HCl, pH 7.5 containing 0.15 M NaCl, 5 mM EDTA, 0.1 mM PMSF, 10 mM benzamidine and 10 mM *N*-ethylmaleimide), separated from matrix by centrifugation and precipitated with 2 M NaCl. Collagens with acid-labile crosslinks were then extracted from the matrix for 24 h with 0.5 M acetic acid and precipitated with 2 M NaCl. Collagens with mature crosslinks were extracted by pepsin digestion (0.1 mg/ml) for 24 h and precipitated with 2 M NaCl. Procollagens from the media were also digested with pepsin before all fractions were electrophoresed on unreduced 6% SDS-urea-PAGE gels (0.5 M urea).

2.11. Immunofluorescence microscopy

Fibroblasts and osteoblasts were seeded in 2- or 4-well chamber slides (Nunc Technologies, Rochester, NY, USA) and incubated under normal growth conditions, until they reached 70% confluence. Cells were washed with phosphate buffered saline (PBS) and fixed in 4% paraformaldehyde in PBS for 15 min at room temperature. Cells were permeabilized and blocked for 5 min at room temperature in a solution of 0.1% Triton X-100 and 1% bovine serum albumin (BSA) in PBS. All antibody dilutions were made in a solution of 1% BSA in PBS. Cells were incubated with primary antibody for 1 h at 37 °C, washed in PBS and incubated with a secondary antibody solution for 1 h at 37 °C. At the end of the incubations, cells were washed in PBS mounted with Vectashield medium (Vector Laboratories, Burlingame, CA, USA). Immunofluorescence labeling was examined using a Zeiss LSM 510 or LSM 710 scanning confocal microscope (Zeiss Inc., Thornwood, NY, USA) using standard Zeiss operating software. The primary antibody dilutions used were as follows: Anti-BiP/Grp78 (Stressgen SPA-827, San Diego, CA, USA) was used at 4 μg/ml, anti-Calnexin (Affinity BioReagents MA3-027, Denver, CO, USA), was used at 1:400 dilution of stock ascites, anti-HSP47 (Stressgen SPA-470) was used at 2.4 μg/ml and anti-PDI (Stressgen SPA-891) was used at 3.5 μg/ml. LF-41/LF-42; α1(I) C-propeptide antibodies were the generous gift of Dr. Larry Fisher, NIH [24]. All secondary antibodies conjugated to Alexa-fluor 488 (Thermo-Fisher, Waltham, MA, USA) were diluted 1:250, all secondaries conjugated to Alexa-fluor 555 were diluted 1:200, and all secondaries conjugated to Alexa-fluor 594 were diluted 1:100 in PBS containing 1% BSA.

2.12. In vitro assays of procollagen processing by BMP-1

^{3}H-tryptophan labeled secreted procollagens were prepared from cultured fibroblasts and their specific activities (6.7 to 8.7 × 10^{6} cpm/mg procollagen) determined after removal of radioactively labeled fibronectin as previously described [25]. Endogenous PCPE-1 was inactivated by acidification (addition of 1 M acetic acid to a final concentration of 0.2 M and incubation at 4 °C for 2 h) followed by readjustment to pH 7.5 (addition of 1 M Tris-HCl pH 8.5 to a final concentration of 0.22 M). BMP-1 activity was then determined as previously described [25,26]. Briefly, 2 μg procollagen (22 nM; 15,000–19,000 cpm) in 200 μl of 0.05 M Tris-HCl, 0.15 M NaCl, 5 mM $CaCl_2$, pH 7.5 were incubated with either 37 or 55 ng BMP-1 (2.3 or 3.4 nM for control or mutant procollagens, respectively) with and without PCPE-1 (100 ng; 10 nM) for either 60 (control) or 120 min (probands). Under these conditions measurements were made within the linear range of the reaction, *i.e.*, only initial rates are determined. The reaction was stopped with EDTA and the free radioactive C-propeptide was separated from un/partially digested procollagen by selective ethanol precipitation. Radioactivity in the C-propeptide-containing supernatants was determined using a Packard Tri-carb 1600 CA β-counter and normalized to an incubation time of 120 min and BMP-1 concentration of 3.4 nM. Radioactivity in cpm was converted to pmole C-propeptide based on the specific activity of each procollagen preparation and assuming that radiolabeled tryptophan is incorporated exclusively into the C-propeptide domain and that the molecular mass of the C-propeptide (100,000 Da) represents 22% of the mass of full-size procollagen (450,000 Da). In a gel assay of C-terminal procollagen processing by BMP-1 [25], procollagen (8000 cpm, ~1 μg; 55.6 nM) was incubated with BMP-1 (5 ng, 1.8 nM) with or without PCPE-1 (50 or 100 ng, 27 or 55 nM, respectively) for 120 min in 40 μl of buffer. The reaction was stopped by heating in SDS sample buffer followed by electrophoresis on 5.5% SDS-urea-gels then autoradiography and densitometry of the proα1(I) and proα2(I) bands to determine their respective degree of processing. Percent processing was calculated using the formula (A-B) divided by A x 100 where A is proα chain band intensity without BMP-1 (control; 100%) and B is the respective band intensity remaining after processing by BMP-1.

2.13. Dermal fibrils

Dermal punch biopsies from probands and age- and gender-matched

controls were fixed in 2.5% glutaraldehyde for 24 h, then transferred to phosphate buffer. Fixed specimens were treated with 1% osmium tetroxide, then 2% uranyl acetate, followed by infiltration by Spurr's plastic resin. Sections 600–800 Å in thickness were analyzed and photographed by transmission electron microscopy, as described [27].

2.14. Bone fibrils

Bone tissue was fixed in a buffered (0.1 M sodium cacodylate buffer, pH 7.4) 2.0% glutaraldehyde solution for 18 h at 4 °C and decalcified in EDTA. The specimens were cut into small pieces (1–3 mm^3) early in the chemical fixation procedure. The tissue was washed (2 × 30 min) in buffer followed by secondary fixation in a 1% osmium tetroxide solution (Agar Scientific Ltd., UK) diluted in 0.1 M sodium cacodylate, pH 7.4. The tissue was dehydrated through a graded series of ethanols (70–100%) and placed in propylene oxide/Spurr's resin (1:1) before vacuum infiltration in freshly prepared Spurr's resin for 2 days and then a final resin change for polymerization at 60 °C for 18 h. An area encompassing trabecular bone was selected and ultrathin sections were cut on a Reichert-Jung ultramicrotome at 40–60 nm, contrasted using aqueous uranyl acetate for 10 min followed by lead citrate before viewing in the transmission electron microscope [28].

For scanning electron microscopy, bone tissue was fixed in buffered 2.0% glutaraldehyde solution (18 h) at 4 °C. Samples were examined after critical point drying and sputter coating with gold.

3. Results

3.1. Identification of C-propeptide mutations

The C-terminus of *COL1A1* (exons 40–52) was screened in NICHD OI probands with moderate to lethal OI (Table 1) by PCR and Sanger sequencing. Six heterozygous mutations, including 4 novel mutations (**P1**, p.(Trp1275Cys); **P2**, p.(Gly1281Val); **P5**, c.4243_4248 + 2delinsCA (I51 indel); **P7**, p.(Pro1444His)), were identified in the C-propeptide coding region of *COL1A1* (Fig. 1A). The mutations in **P3,** p.(Thr1298Ile), and **P4,** p.(Asp1413Asn), have been previously identified in other OI probands, but not studied biochemically [29–32]. Restriction enzyme digestion of gDNA confirmed the presence of the mutation in each proband (Supp. Fig. S1). In addition, we studied a previously reported mutation (**P6**, p.(Asp1441Tyr)) causing lethal OI [33]. Table 1 shows both the position of the mutation sites relative to the start of the C-propeptide sequence and from the transcript start site (p.). These numbers are related by a difference of 1218. In the text below, the C-propeptide number is shown in parentheses after the p. number.

Five mutations were missense substitutions of highly conserved residues, while one mutation was an insertion/deletion leading to the incorporation of most of intron 51 (Supp. Fig. S1). The indel mutation deleted 4 nucleotides around the exon 51 splice donor site, plus 2 exonic nucleotides near the splice that encode C-propeptide p.Cys1415 (residue 197 of the C-propeptide). P5 fibroblast collagen transcripts were either normally spliced or retained intron 51 (data not shown). The retained intron 51 sequence is in-frame and contains no premature termination codons, resulting in insertion of 42 amino acid residues into the C-propeptide outer petal. Interestingly, the proband's mother had mild OI symptoms and was determined to be a high percentage mosaic carrier (data not shown).

3.2. Genotype-phenotype modeling of the structural effects of the mutations

The crystal structures of the procollagen C-propeptide trimers of procollagens I and III have been shown to be flower-shaped, with a stalk, a base region and three petals [4,14]. We located the sites of the OI missense mutations using the crystal structure of the CPI homotrimer, containing three human proα1(I) C-propeptide chains [4], and also a newly generated model for the CPI heterotrimer based on the homotrimer structure and site-directed mutagenesis data [4] (Supp. Fig. S2). Both the CPI homotrimer crystal structure and the CPI heterotrimer model led to the same conclusions concerning the likely consequences of the mutations.

Two of the substitutions were located in the base region (p.Trp1275(57)Cys, p.Gly1281(63)Val), four in the petal region (p.Asp1413(195)Asn, I51 indel, p.Asp1441(223)Tyr, p.Pro1444(226)His) and one at the junction between these two regions (p.Thr1298(80)Ile).

The mutation of P1 occurs in a highly conserved residue, p.Trp1275(57)Cys, in procollagens I to III that occurs in the β1 strand of the crystal structure which immediately precedes the Ca^{2+} binding loop in the base region (Fig. 1A, B). This residue is not directly involved in inter-chain interactions and projects outwards from the base region where it stacks against the hydrocarbon chain of the neighboring p.Arg1252 (34). The latter residue is adjacent to p.Lys1253(35) which is crucial for PCPE-1 binding [34]. Insofar as mutation to cysteine might perturb a nearby inter-chain disulfide bond (Fig. 1A, B), as well as its proximity to p.Lys1253(35) having a possible effect on PCPE-1 binding, the p.Trp1275(57)Cys substitution could be sufficiently destabilizing to account for the observed severe OI III phenotype (Table 2).

Also in the base region, residue p.Gly1281(63), mutated to valine in P2, is located in a highly conserved loop that provides a Ca^{2+} binding site that is crucial for structural stabilization of this region. Mutation to a large valine residue almost certainly disrupts the Ca^{2+} binding site and perhaps also the formation of a nearby inter-chain disulfide bond (Fig. 1A, B), thus accounting for the observed lethal OI II phenotype (Table 2).

Residue p.Thr1298(80), mutated to isoleucine in P3, is located in the highly conserved β3 strand adjacent to a loop on the outer face of the base/petal junction (Fig. 1A, C). This strand occurs between two closely spaced intra-chain S—S bonds p.Cys1299(81)-p.Cys1462(244) and p.Cys1259(41)-p.Cys1291(73), where the side-chain of p.Thr1298(80) points inwards and interacts closely with p.Cys1259(41). Mutation to isoleucine would disrupt this interaction, thus destabilizing this region leading to the observed moderately severe OI IV phenotype (Table 2).

Table 1
Patient mutations.

Patient ID	Proband #	c.	p.	C-propeptide#	3D Location	Phenotype
AN_002007		c.3226G > A	p.(Gly1076Ser)	–	helix	Severe
AN_002008		c.3433G > T	p.(Gly1145Cys)	–	helix	Severe
AN_002009		c.3523G > A	p.(Gly1175Ser)	–	helix	Severe
AN_002010	P1	c.3825G > T	**p.(Trp1275Cys)**	**57**	base	Severe
AN_002011	P2	c.3842G > T	**p.(Gly1281Val)**	**63**	base, Ca^{2+} binding loop	Lethal
AN_002012	P3	c.3893C > T	**p.(Thr1298Ile)**	**80**	base/petal junction	Moderate
AN_002013	P4	c.4237G > A	**p.(Asp1413Asn)**	**195**	outer petal	Severe
AN_002014	P5	c.4243_4248 + 2delinsCA	**Splice-site**	–	outer petal, del p.Cys1415(197)	Lethal
AN_004605	P6	c.4321G > T	**p.(Asp1441Tyr)**	**223**	inner petal	Lethal
AN_002015	P7	c.4331C > A	**p.(Pro1444His)**	**226**	center petal	Moderate

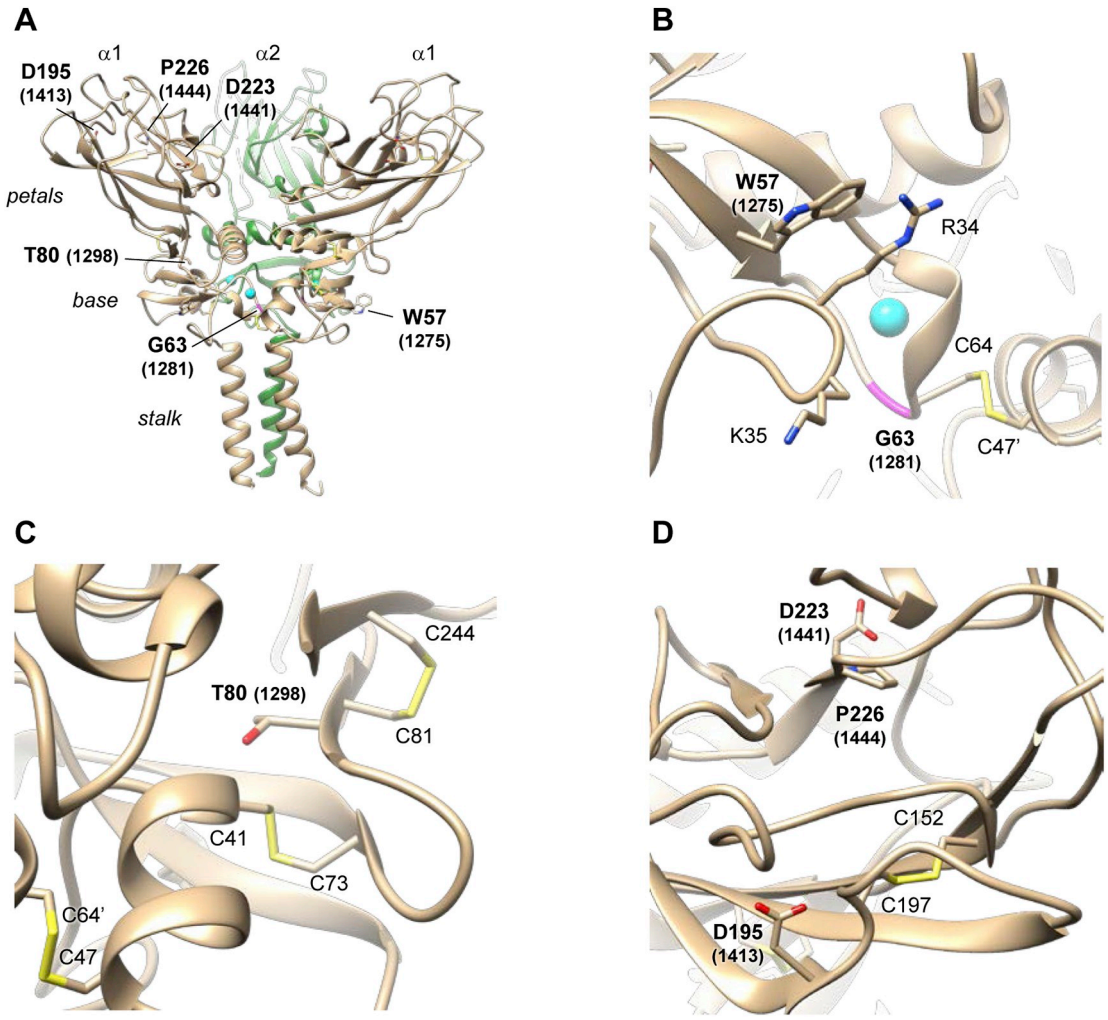

Fig. 1. Structural model of the CPI heterotrimer and positions of mutation sites.
A) Overall structure showing the stalk, base and petal regions, the two α1(I) chains in beige, the α2(I) chain in green, bound Ca^{2+} ions in blue and disulfide bonds in yellow. Mutation sites are indicated (in **bold**) for one of the two α1(I) chains. Residues are numbered from the N-terminus of the C-propeptide after cleavage from the rest of the molecule, as well as from the transcription start site of the full-length chain (in parentheses). B) Close-up of W57(1275), G63(1281) and other residues in the base region. C) Close-up of T80(1298) and neighboring disulfide bonds at the base/petal junction. D) Close-up of D195(1413), D223(1441) and P226(1444) and a nearby disulfide bond in the petal region. Residues marked with an apostrophe (') refer to adjacent chains in the trimeric structure.

The four remaining mutations were found in the outer part of the petal region and thus far from the inter-chain interfaces (Supp. Fig. S2 and Fig. 1A, D). The highly conserved residue p.Asp1413(195), mutated to asparagine in P4, occurs on the outer face of the petal, close to the p.Cys1415(197)-p.Cys1370(152) disulfide bond, where it makes weak interactions with its neighbors. Though these interactions will be perturbed by mutation to asparagine, this mutation would not be expected to cause the severe OI III phenotype (Table 2). Another aspartate mutation, p.Asp1441(223)Tyr, corresponds to a highly conserved residue on the inner face of the petal (Fig. 1A, D), which also makes weak interactions with its neighbors. Since mutation to tyrosine could probably be accommodated without major structural changes, it also seems surprising that this leads to a lethal phenotype [33] (Table 2, see Discussion). Residue p.Pro1444(226), mutated to histidine in P7 is located nearby. This is also a highly conserved residue, located on the inner face of the petal (Fig. 1A, D), where it interacts with the hydrophobic core. Because of these interactions and the role of proline in providing rigidity, it is likely that mutation to histidine will be destabilizing, consistent with the moderate OI IV phenotype (Table 2). Finally, the I51 indel mutation also occurs in this part of the petal, resulting in a 42 residue sequence insertion that will have major structural consequences leading to the observed lethal OI II phenotype (Table 2).

3.3. Effects of C-propeptide mutations on collagen modification

To understand how changes in the C-propeptide affect collagen biochemical properties, the steady-state modification of pepsinized procollagens containing C-propeptide mutations was compared to collagen with glycine substitutions near the carboxyl-end of the collagen helix (Fig. 2A). Collagens from probands with C-terminal helical mutations and C-propeptide mutations showed varying extents of overmodification in secreted and cell layer collagens. Additionally, all C-propeptide probands except P6, with p.Asp1441Tyr, had a population of normally migrating α1(I) chains. Gel electrophoresis of collagen from several probands including P1, P3, P5, (p.Trp1275Cys, p.Thr1298Ile and I51 indel, respectively) as well as helical p.Gly1076Ser (helical residue Gly898), showed a "backstreaking" appearance, indicative of overmodification. Overmodified collagen was relatively more retained intracellularly than secreted from P4, P5, P6 and P7 (p.Asp1413Asn, I51 indel, p.Asp1441Tyr and p.Pro1444His, respectively). These data suggest that delayed triple helical folding may contribute to collagen overmodification. This was supported by intracellular folding assays, which detected ≈65% of fully folded collagen in cells with the p.Trp1275Cys, p.Gly1281Val and p.Thr1298Ile substitutions *vs* 100% for control cells at 30 min (Supp. Fig. S3).

Table 2
Clinical Information.

Mutation	OI Type	Current Age (y)	Height Age#	Scoliosis	HC#	Scleral Hue	Teeth	Functional Status	DXA Z-score	Fractures	Limb Deformities/Rods
p.Gly1175Ser	III	$9\ ^{3}/_{12}$	50% for 24 mo	None apparent	50% for age	2+	+DI; orangey brown	Manual w/c, occasionally uses walker	−5.2	Multiple LE & UE	BL femur/tibiae & R humerus rods; UE/LE sig bowing
p.Trp1275Cys	III	$11\ ^{10}/_{12}$	32.25 in.	40° thoracic, progressive	Normo-cephalic	"blue"	mild DI	w/c	−2.3*	> 100 in lifetime	Multiple rodding procedures
p.Gly1281Val	II				Clinical details not available on lethal infant.						
p.Thr1298Ile	IV	17	50% for 4½ y male	62°	2% age; 50% for 10 y	1	mild DI	Walks with walker & brace; otherwise uses manual w/c	−5.7	3 LE fx over lifetime	R tib rod; R femur chronic nonunion; UE/LE sig bowing
p.Asp1413Asn	III	$7\ ^{5}/_{12}$	At 5½ y, 50% for 19 mo girl	Minimal curve	At 5½ y, 50% for 3 y	2	+DI, grey-blue	Primarily w/c, occasional walking with walker	−5	Multiple LE	BL femurs
I51 indel	II				Clinical details not available on lethal infant.						
p.Pro1444His	IV	$14\ ^{1}/_{12}$	At 10 y, 50% for 6 y girl	5–10°	At 10 y, 54.5 cm	1	No DI	Ambulatory; uses crutches	−3.79	About 6 femur fx, mostly LE	BL femurs/BL tibs rodded

Abbreviations: y = years; mo = months; HC = head circumference; w/c = wheelchair; DI = dentinogenesis imperfecta; LE = lower extremity; UE = upper extremity; BL = bilateral; R = right; sig = significant.
* = Patient has been treated with pamidronate, # = % refers to the percentile of children of the same age who have this measurement; 50% refers to the age at which an average child would have this measurement.

To further explore the relationship of collagen folding and modification in the context of C-propeptide mutations, we analyzed the hydroxylysine content of the helical region of six of the mutant collagens (Supp. Table 1) as well as normal control and controls with mutations at the C-terminal end of the helix. We found that the collagen helices of trimers with C-propeptide mutations do have increased hydroxylysine content (26–36% hydroxylysine/total lysine) compared to normal controls (22–25% hydroxylysine/total lysine), but to a lesser extent than caused by mutations near the carboxyl end of the helix (38–40% hydroxylysine/total lysine). Furthermore, there was no direct correlation between the extent of lysine hydroxylation and the extent of the collagen backstreaking present on gel electrophoresis, a measure of both lysine hydroxylation and subsequent glycosylation.

Differential scanning calorimetry of collagen with substitutions in the base (p.Trp1275Cys, p.Gly1281Val) or base/petal junction (p.Thr1298Ile) as well as procollagen with substitutions in the petal (p.Asp1441Tyr and p.Pro1444His) revealed normal thermal stability (Fig. 2B). In contrast, the collagens with helical mutations near the C-propeptide showed large decreases in thermal stability (Supp. Fig. S4) [19]. Collagen 3-hydroxylation from two C-propeptide probands (p.Thr1298Ile, p.Pro1444His) was normal (97–98%).

3.4. Proband procollagen assembly is delayed

Procollagen chain association has previously been shown to be delayed in cells with C-propeptide mutations [33,35,36]. All cell lines in this report with C-propeptide mutations, even the most C-terminal, showed delayed proα1(I) incorporation (Supp. Fig. S5), most to 120 min, in comparison to control fibroblasts in which proα1(I) displayed 50% incorporation by 20 min post-chase. This was particularly striking for mutations in the petal region (I51 indel, p.Asp1441Tyr, p.Pro1444His). Only cells with the lethal α1(I)p.Gly1281Val substitution, flanked by Ca^{2+}-interacting residues, had a shorter incorporation delay of about 60 min. Interestingly, the helical mutation closest to the C-propeptide also delayed chain incorporation.

Comparison of extent of delay in chain association with the proportion of helical hydroxylysine content or extent of backstreaking on gel electrophoresis did not yield direct correlations with either measurement, suggesting that delay in chain association is not the sole determinant of collagen overmodification.

3.5. Procollagen chains with C-propeptide mutations are mislocalized in ER lumen

Assembly of procollagen chains into trimers takes place at the rough endoplasmic reticulum (rER) membrane [37]. We investigated whether C-propeptide mutations affected procollagen localization. Immunofluorescent staining of fibroblasts with p.Gly1076Ser and p.Gly1175Ser substitutions (helical Gly898 and Gly997 residues, respectively) using a C-propeptide antibody colocalized with the ER-membrane chaperone calnexin (Fig. 3A, Supp. Fig. S6). In contrast, collagen with C-propeptide mutations (p.Trp1275Cys, p.Thr1298Ile, p.Pro1444His) show an ER luminal staining pattern of the C-propeptide, colocalizing with ER chaperones PDI, BiP, and HSP47 (Fig. 3A, Supp. Fig. S6A). Mislocalization of mutant procollagen was especially prominent for cells with mutations in the C-propeptide petal region (p.Asp1413Asn and p.Asp1441Tyr, Fig. 3B). In these cells, globular aggregates of procollagen were detected in the ER lumen.

Altered C-propeptide localization to the ER lumen was also confirmed in osteoblasts from one C-propeptide proband (p.Pro1444His) (Fig. 3C, Supp. Fig. S6B). As previously demonstrated [38], BiP appears increased only in C-propeptide probands (Supp. Fig. S6A).

3.6. Procollagen C-propeptide processing is decreased

Given the proximity of some C-propeptide mutations to the C-

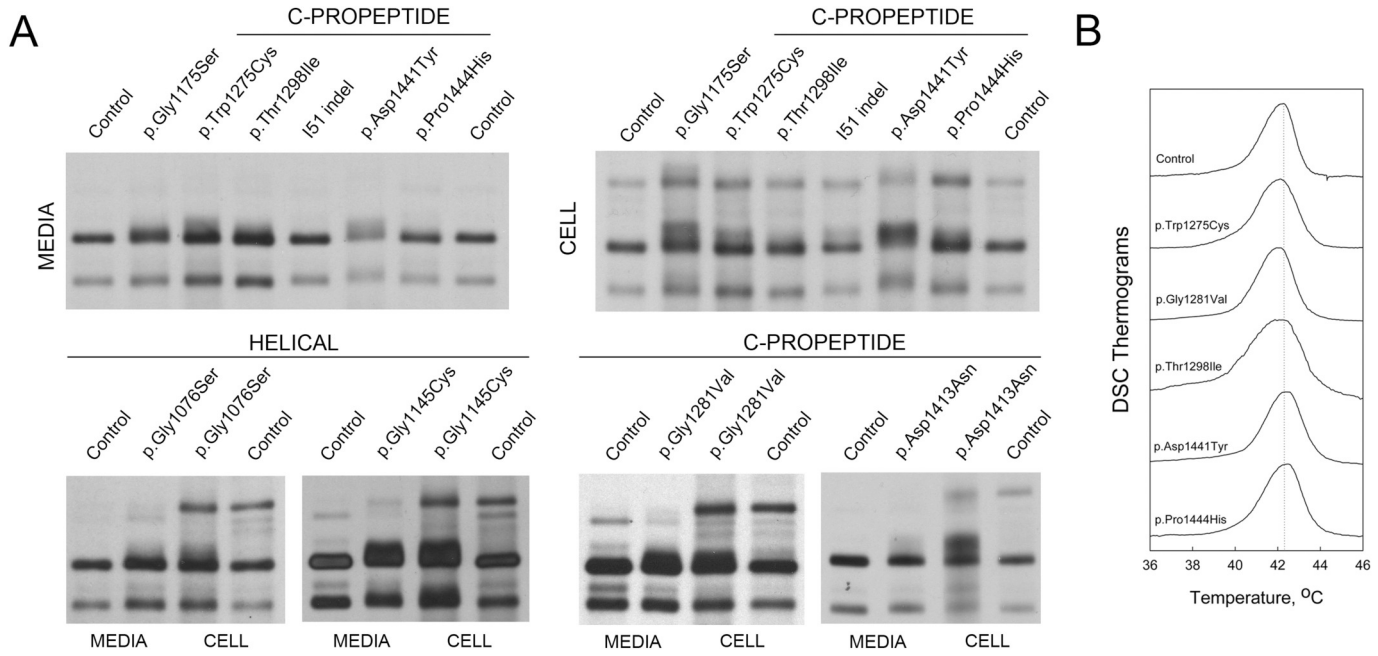

Fig. 2. Probands with C-propeptide mutations have overmodified steady-state collagen protein.
A) Autoradiography of type I collagen chains from all probands shows backstreaking or overmodification of the α1(I) and α2(I) chains on SDS-urea-PAGE; slower migrating forms were more prominent in the cell fraction. B) Differential scanning calorimetry of C-propeptide probands' collagens shows normal thermal stability.

propeptide cleavage site, they might alter C-propeptide folding and decrease the binding of BMP-1 or PCPE-1 to the C-propeptide. Therefore, we monitored procollagen processing in both pericellular and *in vitro* assays.

In pericellular assays, proband fibroblasts all displayed abnormal processing. Substitutions p.Trp1275Cys (base region), I51 indel, p.Asp1441Tyr, and p.Pro1444His (all petal region), led to a prominent increase in both pC-α1 and pC-α2 over 5 days, but mature collagen was seen on the final days of the assay (Fig. 4A). This increase in pC was also seen for p.Gly1281Val (base), p.Thr1298Ile (base/petal junction), and p.Asp1413Asn (petal), but with very low levels of mature collagen, even after 5 days (Fig. 4A). Interestingly, late helical substitutions also displayed slower processing with accumulation of overmodified collagen in pC-forms.

In vitro cleavage assays to quantify the rate of release of radiolabeled C-propeptides from five of the mutant procollagens, using purified BMP-1 ± PCPE-1, showed that the activity of BMP-1 for the probands' procollagens was 60–70% lower than the control (Table 3, Fig. 4B). Enhancement of BMP-1 activity by PCPE-1 was similar to control, but slightly decreased for p.Gly1281Val and p.Thr1298Ile (Table 3). Cleavage of individual proα chains was also examined by gel electrophoresis (Table 4, Fig. 4C). With BMP-1 alone, the extent of processing of both proα1(I) and proα2(I) was 30–40% lower than the controls except for p.Thr1298Ile, which showed normal cleavage of both chains. Enhancement by PCPE-1 was similar to that seen in the quantitative assays (Table 3), with substantially lower enhancement in p.Thr1298Ile (Table 4). It should be noted that these assays measure two different parameters, either release of C-propeptide trimers (kinetic assay, Table 3) or cleavage of individual procollagen chains (gel assay, Table 4; Fig. 4C), hence the differences in the percentage changes in activity.

3.7. C-propeptide incorporation into extracellular matrix alters fibrils in dermis and bone

Next, we examined whether collagen processed from mutant procollagen was incorporated into matrix deposited in culture. Collagen present in matrix shows backstreaking of the neutral salt fractions and diffuse backstreaking in the mature, cross-linked fraction (pepsin fraction, Fig. 5), although less than in the collagen secreted into the media. In addition, there are bands at the level of pC-collagen in the acetic acid fractions of 6 of the 7 cases with C-propeptide mutations. In 4 of the 7 cases, the pC-collagen bands are quite prominent; only the p.Gly1281Val deposition does not have such bands. Interestingly, the pC-collagen band was also prominent in p.Gly1175Ser at the extreme end of the helical region that has some properties, such as delayed chain assembly, in common with the C-propeptide mutations. In contrast, amounts of pN-collagen were similar to controls.

Incorporation of mutant pC-collagen also affects fibril diameters in dermis and bone. Comparison of dermal fibril diameters from two C-propeptide probands and one classical OI proband with age-matched controls revealed that proband dermal fibrils have a round cross-section and regular borders. Cauliflower forms and barbed wire appearance were not seen. However, the fibril diameters of p.Pro1444His were significantly increased ($p \ll 0.01$), with normal variability (Fig. 6A). In contrast, the fibril diameters of the helical p.Gly1175Ser (Gly997 of helix) and p.Thr1298Ile probands were not significantly different from age and gender matched controls, although both had significantly increased variability ($p \ll 0.01$, $p = 0.016$, respectively).

Bone fibrils from the p.Thr1298Ile and p.Pro1444His probands were also examined. Proband bone fibrils showed a normal D-period banding pattern. Fibrils had a wide variation in size, both between and within individual fibrils, and appeared disorganized (Fig. 6B).

4. Discussion

We report here biochemical investigations on cells and purified collagen from seven probands with moderate to lethal OI who have mutations in the *COL1A1* C-propeptide, in comparison to classical glycine substitutions in the collagen helix. We found that collagen from the probands' cells is overmodified, likely due to a combination of delayed chain association and slow helical folding, but has normal thermal stability, in agreement with previous studies of defective procollagen C-propeptides [35,36,39].

The clinical consequences of these mutations can be compared to the relatively milder phenotype of patients with mutations at the C-

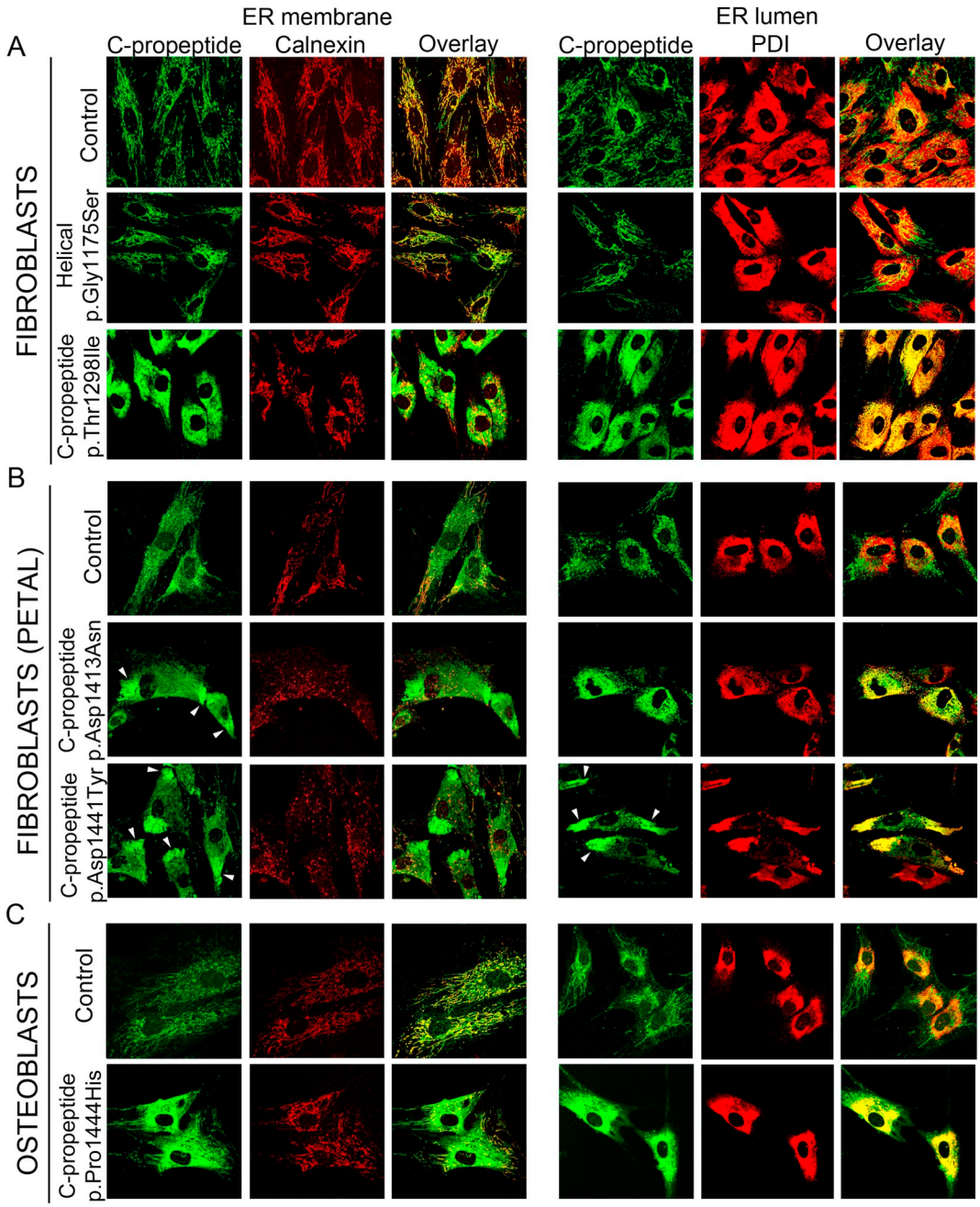

Fig. 3. Procollagen with C-propeptide mutations dissociates from the rER membrane and localizes to the ER lumen.
A) Immunofluorescence microscopy shows colocalization of the C-propeptide and the ER membrane-bound chaperone calnexin in control fibroblasts and fibroblasts from a patient with the helical mutation p.Gly1175Ser. C-propeptide (p.Thr1298Ile) proband fibroblasts show decreased overlap of the C-propeptide with calnexin and an increased overlap with the ER luminal chaperone PDI. B) Immunofluorescence microscopy of fibroblasts with mutations in the petal region of the C-propeptide shows large C-propeptide aggregates (white arrowheads) in a few (p.Asp1413Asn) or in most cells (p.Asp1441Tyr), that strongly colocalized with PDI. C) Immunofluorescence microscopy of p.Pro1444His osteoblasts confirms ER luminal localization of the C-propeptide and increased overlap with PDI.

propeptide cleavage site, who presumably have normal C-propeptide structure [25]. Previous genotype-phenotype modeling of C-propeptide mutations showed that the most severe phenotypes were associated with substitutions localized at the distal end of the C-propeptide primary sequence, or in regions that disrupt inter-/intra-chain disulfide bonds, internal hydrophobic interactions or calcium binding, while milder mutations are located at the surface with few interactions [13,14]. We mapped the substitutions on the crystal structure derived from the CPI homotrimeric C-propeptide [4], as well as on a structural model of the CPI heterotrimer. Some probands, with the most severe phenotypes, have substitutions (p.Trp1275Cys, I51 indel, p.Gly1281Val) that affect disulfide bonds or calcium binding, respectively, in agreement with the model. The predictions of the structure-based modeling could be tested using recombinant CPI [4] mutated at the corresponding sites, probing for changes in disulfide bonding using mass spectrometry [5] or studying changes in calcium binding using Ca^{45} incorporation [40]. In contrast, the substitutions p.Asp1413Asn and p.Asp1444Tyr are surface located, in the petal regions, and their localization in the C-propeptide structure did not predict their lethal/severe phenotype.

We present the novel observation that, unlike the normal localization of procollagens with helical mutations to the ER membrane on

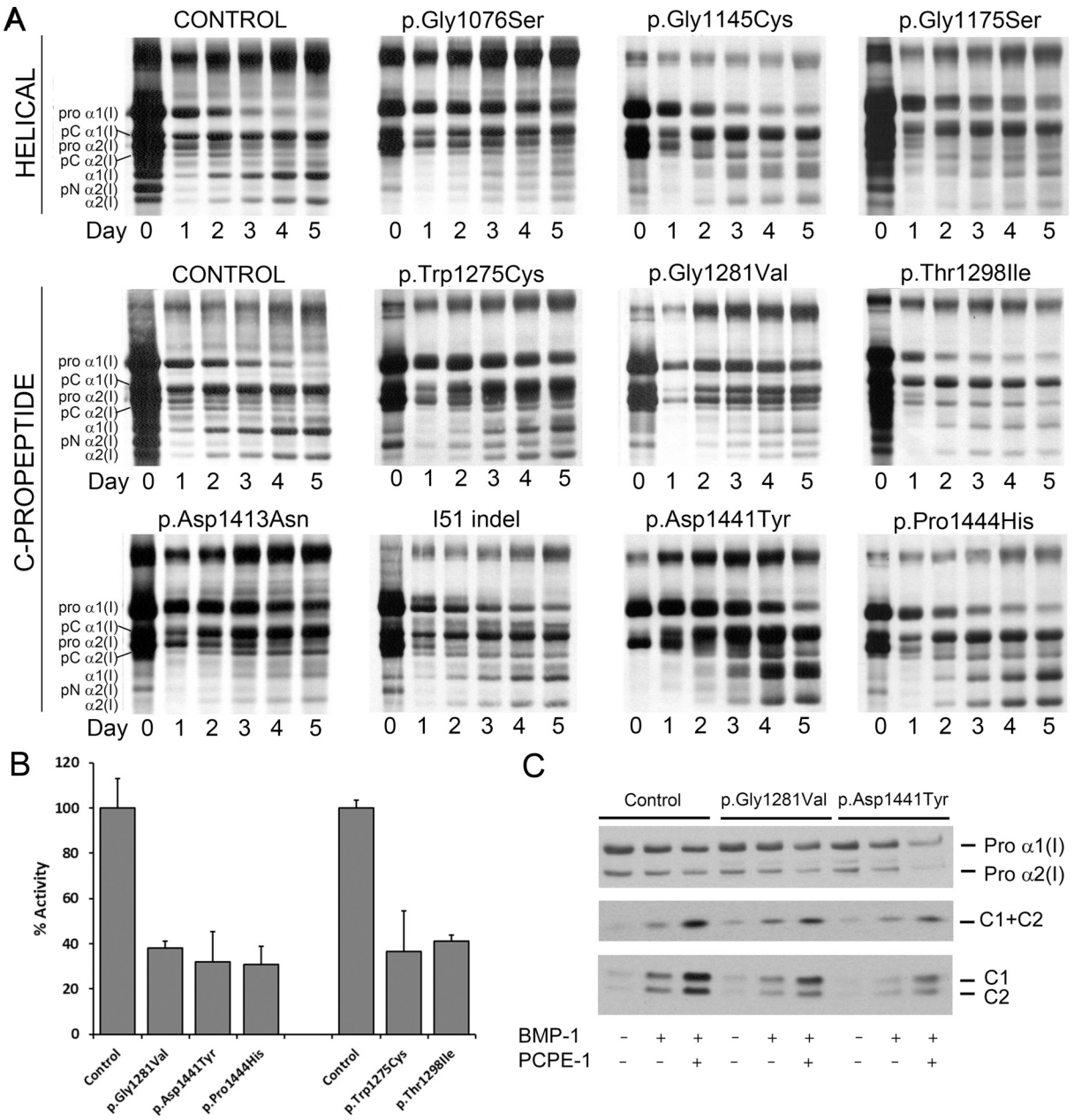

Fig. 4. Probands with C-propeptide mutation have defective processing of procollagen.
A) Pericellular processing of secreted procollagen by control cells shows an increase of mature α1(I) and α2(I) and a concomitant decrease of pro α1(I) starting at Day 2. Probands with mutations in the C-propeptide or the carboxyl end of the collagen helix have a delay in pro α1(I) processing and an increased proportion of pC-α1(I) collagen compared to control. Additionally, mature collagen is often much less abundant than control. B) Processing of the trimeric C-propeptide by BMP-1 from probands' procollagens compared to controls (based on Table 3; BMP-1 alone). BMP-1 can only fully cleave 30–40% of the trimeric C-propeptide from probands' procollagens compared to cleavage of control procollagens (data are normalized to 120 min incubation). C) Representative autoradiogram shows that processing of the pro-α chains from p.Gly1281Val and p.Asp1441Tyr by BMP-1 is reduced. Top and central panels, 6% gel, reduced. The C-propeptide subunits, C1 and C2, are not resolved and appear as a single band (designated C1 + C2) representing the total amount of the C-propeptide released. Bottom panel, 12% acrylamide gel, reduced where the C-propeptide subunits, C1 and C2, are resolved.

immunofluorescence, procollagen with C-propeptide substitutions is mislocalized in the ER lumen suggesting that the misfolded C-propeptide can no longer bind to the rough endoplasmic reticulum to coordinate proper folding and modification [37,41]. Disruption of these interactions provides a functional rationale for the clinical severity of the surface-associated C-propeptide mutations p.Asp1413Asn and p.Asp1441Tyr which give rise to severe or lethal phenotypes, and are associated with delayed assembly (Supp. Fig. S5). In addition, mislocalization of procollagen with C-propeptide defects may also affect its packaging into COPII-like secretory vesicles and subsequent trafficking to the Golgi for secretion, or may hinder its recruitment by cargo adaptors [42]. Mislocalization in the ER lumen of procollagen with C-propeptide mutations may also contribute to the differences in collagen lysine hydroxylation and subsequent glycosylation as reflected in backstreaking on gel electrophoresis. The lack of direct correlation between any two of chain assembly delay, lysine hydroxylation and gel backstreaking, as well as the intermediate overmodification between normal controls and helical collagen mutations, suggests that the collagen modifying enzymes may have reduced access to the mutant chains, which would be a reasonable result of ER mislocalization.

Table 3
Procollagen processing as measured by the release of the radioactively labeled C-propeptide trimer.

	BMP-1 alone		BMP-1 + PCPE-1		PCPE-1 Enhancement
Procollagen	pmole C-Pro	Relative activity (%)	pmole C-Pro	Relative activity (%)	A/A_o
Control	0.39 ± 0.05	100 ± 13.0	1.28 ± 0.08	100 ± 5.9	3.3
p.Gly1281Val	0.13 ± 0.01	33 ± 2.6	0.35 ± 0.03	27 ± 1.1	2.7
p.Asp1441Tyr	0.12 ± 0.02	31 ± 4.0	0.44 ± 0.09	34 ± 6.8	3.7
p.Pro1444His	0.11 ± 0.01	28 ± 2.2	0.34 ± 0.01	27 ± 0.2	3.1
Control	0.29 ± 0.01	100 ± 3.3	1.13 ± 0.03	100 ± 2.2	3.9
p.Trp1275Cys	0.12 ± 0.02	41 ± 18.3	0.48 ± 0.09	42 ± 18.3	4.0
p.Thr1298Ile	0.12 ± 0.01	41 ± 3.3	0.28 ± 0.01	25 ± 5.0	2.3

Values in pmoles are means ± SD, normalized to 2 h of incubation and 3.4 nM BMP-1. $n = 4$ except for p.Thr1298Ile where $n = 2$.

We further report here the novel finding that procollagen from our C-propeptide probands has decreased C-propeptide processing in both pericellular and *in vitro* assays, with matrix deposition of pC-collagen in 6 of 7 cases. Defects in the C-propeptide cleavage site have been shown to cause high bone mass OI [25]. Furthermore, deficiency of the predominant procollagen C-proteinase, BMP-1, also causes OI [43]. Mild disturbance of type I procollagen processing was previously noted on gel electrophoresis of fibroblast collagen from one proband with both a *COL1A1* p.Asn1394Ser C-propeptide substitution and a *COL1A2* exon 14 skipping defect [13,44]. In that case, the OI/EDS phenotype and increased pN-collagen are more indicative of a processing defect of the N-propeptide than of the C-propeptide. In the probands presented here, pericellular processing assays show an increase in the presence of pC-collagen and a decrease in mature processed collagen, suggesting mutant procollagen prevents proper cleavage of the C-propeptide in a cellular environment. Similar to high bone mass OI caused by lack of C-propeptide cleavage, the p.Asp1441Tyr proband had dense bones [33].

Conversion of procollagen to collagen occurs in a step-wise process at the C-propeptide cleavage site. This apparently begins with random cleavage of a proα1(I) or proα2(I) chain (or the respective pC-α chains that contain the C-propeptide but lack the N-propeptide), followed by proα2(I) cleavage if still unprocessed, and ends with cleavage of the second proα1(I) chain [45,46]. In our *in vitro* assays with BMP-1 (Table 3), only about one-third of trimeric C-propeptides were fully released from mutant procollagens relative to control. For these heterozygous mutations, given that 25% of the C-propeptide trimers contain only normal pro α1(I) chains, this is consistent with release of mainly normal C-propeptide trimers together with small amounts of trimers containing one or two mutant chains. In addition, as shown by SDS-PAGE and densitometry of proα chains from probands with C-propeptide mutations (Table 4), at least two-thirds of the total proα1(I) chains (50% of which are normal) were cleaved, compared to controls, again consistent with release of mainly normal proα1(I) chains together with small amounts of mutant chains. Interestingly, with the exclusion of p.Thr1298Ile (Table 3, Table 4), enhancement by PCPE-1 of BMP-1 cleavage of mutant procollagens was not affected. This suggests that most mutations do not alter binding of PCPE-1 to the C-propeptide, despite the close spatial proximity of p.Trp1275(57)Cys to p.Lys1253(35), one of the critical residues for PCPE-1 binding [34]. It is not clear, however, how the p.Thr1298Ile(80) mutation affects PCPE-1 enhancement, as this is far from its known binding sites, but it may induce long-range structural changes that hinder the mechanism of action of PCPE-1.

The *Bmp1*$^{-/-}$/*Tll1*$^{-/-}$double knockout mouse, which cannot cleave type I procollagen, forms “barbed-wire”-like collagen fibrils in skin from incorporation of pC-collagen [47]. Although we found increased pC-collagen in patient matrix acetic acid fractions, the “barbed-wire” appearance was not found in skin fibrils of the two C-propeptide probands examined (p.Thr1298Ile, p.Pro1444His), perhaps because C-propeptide cleavage is not totally blocked in the heterozygous patients, as it is in the homozygous mice. We observed round fibrils with normal to slightly increased diameter and increased variability in p.Thr1298Ile, in comparison to the irregular fibril cross-sections seen with C-propeptide cleavage site mutations [25]. Skin fibrils with an α1(I) cleavage site mutation also lacked a “barbed-wire” appearance, had normal mean diameters and increased variability [25]. Although the unavailability of pediatric bone controls precludes quantitative analysis, fibrils in C-propeptide proband bone from a C-propeptide proband were irregular in size, even along individual fibrils, and the fibrils were disorganized overall. The increased collagen production in bone tissue *vs* skin dermis may exacerbate the incorporation of pC-collagen into fibrils.

C-propeptide cleavage deficiency also affects the availability of the C-propeptide trimer for cell signaling in bone formation. In osteoblasts, trimeric type I collagen C-propeptides have been reported to be involved in negative feedback regulation of collagen gene expression, in promotion of cell attachment through integrins and in enhancement of TGF-β signaling [48–51]. The C-propeptide released from type II

Table 4
Procollagen processing *in vitro* as measured by densitometry after SDS-PAGE and autoradiography.

	BMP-1 alone Pro α1		BMP-1 + PCPE-1 Pro α1		Pro α1 A/A_o	BMP-1 alone Pro α2		BMP-1 + PCPE-1 Pro α2		Pro α2 A/A_o
Procollagen	% processing ± SD	Relative activity (%)	% processing ± SD	Relative activity (%)		% processing ± SD	Relative activity (%)	% processing ± SD	Relative activity (%)	
Control	23.3 ± 1.5	100 ± 6.4	67.3 ± 4.6	100 ± 7	2.9	26.4 ± 1.9	100 ± 7	67.2 ± 4.5	100 ± 7	2.6
p.Gly1281Val	14.9 ± 2.0	63 ± 13.4	34.1 ± 6.3	51 ± 18	2.3	17.0 ± 2.5	64 ± 9	38.5 ± 7.5	57 ± 11	2.3
p.Asp1441Tyr	14.7 ± 1.7	63 ± 11.6	49.4 ± 7.2	73 ± 15	3.4	18.0 ± 2.0	68 ± 7	53.0 ± 14.0	79 ± 21	2.9
p.Pro1444His	15.5 ± 2.9	66 ± 18.7	47.0 ± 11.0	70 ± 23	3.0	14.5 ± 1.3	55 ± 5	47.0 ± 11.0	70 ± 16	3.2
Control	23.5 ± 2.2	100 ± 9.4	81.2 ± 4.3	100 ± 5	3.5	32.4 ± 3.5	100 ± 10	63.8 ± 3.8	100 ± 6	2.0
p.Trp1275Cys	19.5 ± 5.3	83 ± 22.5	64.4 ± 13.0	79 ± 20	3.3	23.2 ± 3.1	83 ± 11	54.2 ± 3.6	85 ± 6	2.3
p.Thr1298Ile	25.7 ± 3.2	109 ± 13.6	46.5 ± 6.4	57 ± 14	1.8	34.8 ± 5.2	107 ± 16	48.3 ± 10.8	76 ± 17	1.4

Values are means ± SD. Top: Values for each procollagen are from two independent experiments and 4–6 OD measurements for each pro-α chain per experiment. Bottom: Values for the control and p.Trp1275Cys procollagens are from three independent experiments and 3–4 OD measurements for each pro-α chain. Values for p.Thr1298Ile are from one experiment and 2 and 4 OD measurements for pro-α1 and pro-α2, respectively. A and A_o, Activity with and without PCPE-1, respectively.

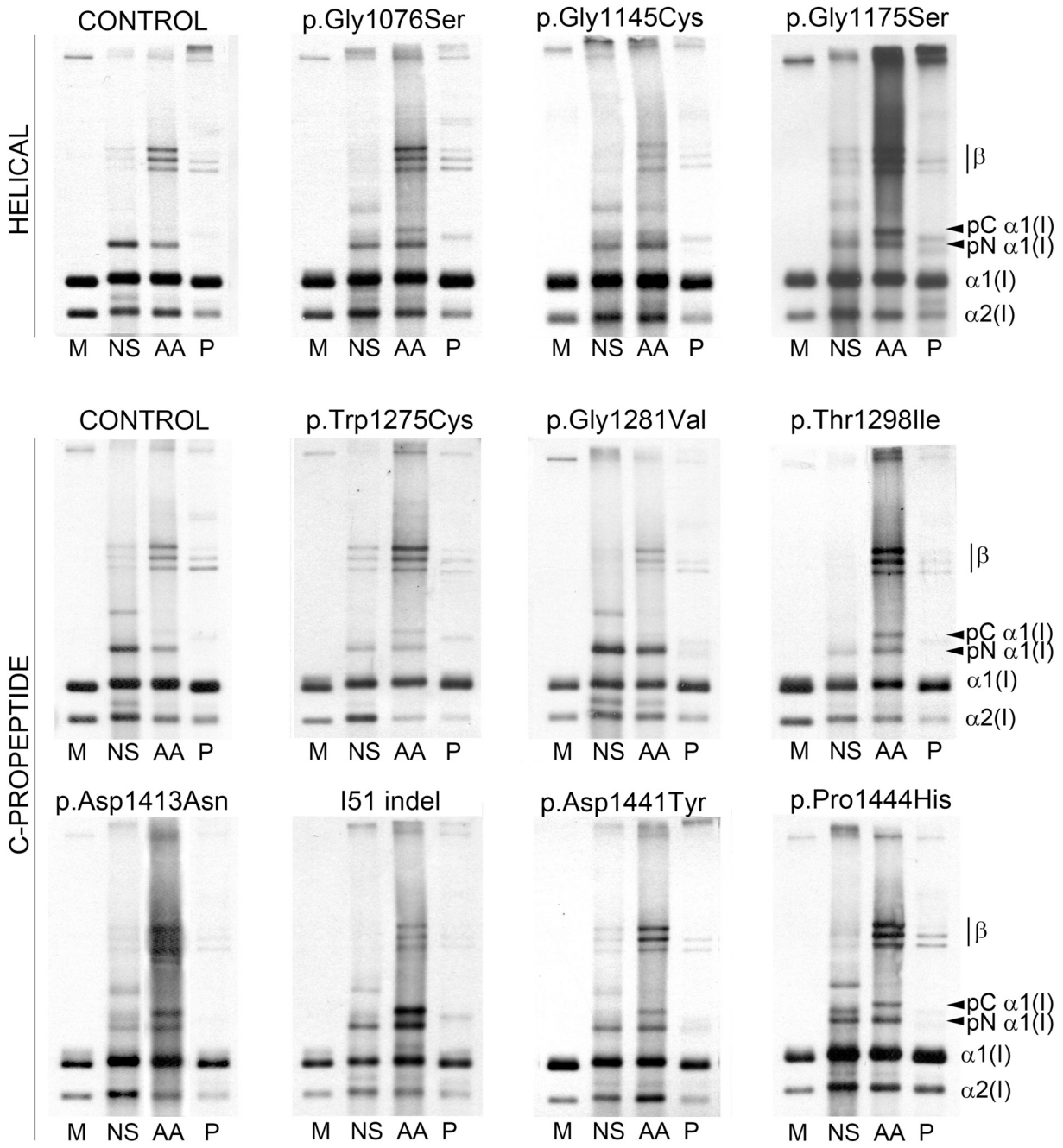

Fig. 5. Collagens with C-propeptide mutations are deposited into the extracellular matrix and form mature cross-links.
Mature cross-linked collagen from matrix deposited in culture (P) shows overmodification and backstreaking similar to secreted collagen (M). Helical mutations show an overall broadening of all matrix fractions, suggesting that a higher proportion of mutant collagen is being secreted and incorporated into the extracellular matrix. Increased levels of pC-collagen α1(I) are observed in the matrix of several probands in immature matrix fractions (AA). M: media/secreted collagen, NS: neutral salt extraction/newly incorporated collagen without cross-links, AA: acetic acid extraction/immaturely cross-linked collagen, P: pepsin extraction/fully cross-linked collagen.

procollagen, chondrocalcin, provides a precedent for a transcription repressor function, as it inhibits its own gene expression *via* a negative feedback mechanism [52,53]. Both type I and type II C-propeptide trimers have been shown to be taken up into the cell [52,54]. Thus, it is tempting to speculate that a decrease in C-propeptide trimer released from type I procollagen, its structural alteration, or mislocalization in the ER, would affect collagen gene transcription and osteoblast function, further contributing to their OI pathology.

Initiation of collagen mineralization occurs at the gap region on the collagen fibril. Retained type I C-propeptides would localize at these gap regions and may create additional nucleation sites along the fibril for bone mineralization. One possible mechanism would involve excess recruitment of matrix vesicles. Secreted from mineralizing cells, matrix vesicles are proposed to play a role in establishing the initial deposition of bone mineralization [55]. Matrix vesicles contain Ca^{2+} and P_i for initial formation of hydroxyapatite, in addition to a myriad of enzymes, proteins and RNAs that promote the mineralization process. Notably, the lipid layer of matrix vesicles is enriched with sphingomyelin, which interacts with C-propeptides [56]. Thus, the retained C-propeptide on fibrils may engage excess matrix vesicles and contribute to the hypermineralization in OI with defective C-propeptide processing.

In summary, we have shown that mutations in the C-propeptide and

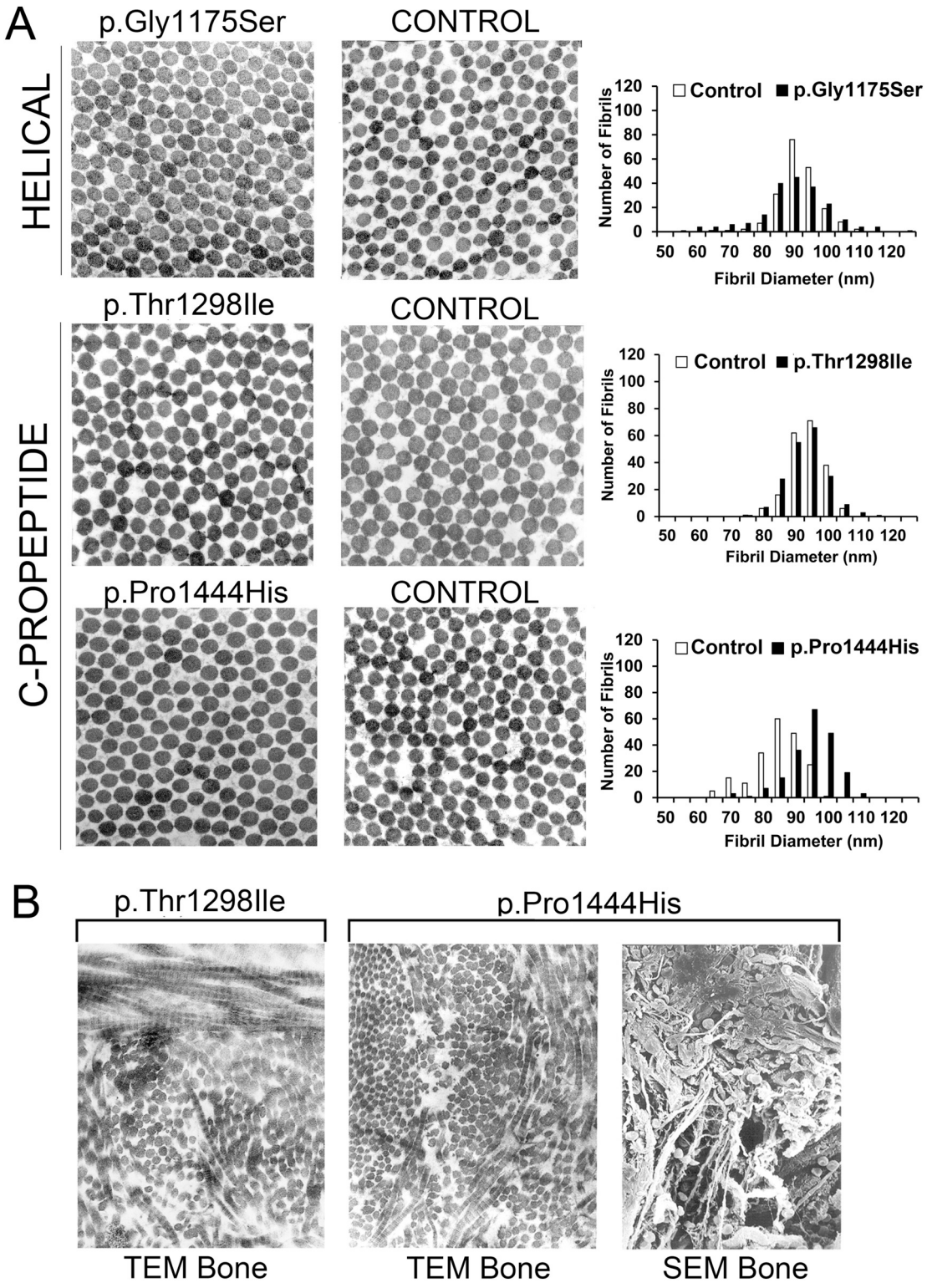

Fig. 6. Fibrils from C-propeptide probands have round cross-sections and increased disorganization in bone.
A) Dermal collagen fibrils from one helical proband (p.Gly1175Ser) and two C-propeptide probands (p.Thr1298Ile, p.Pro1444His) were examined by transmission electron microscopy (TEM) and compared with age and gender matched controls (n = 200). All probands have round fibrils, without irregular forms. p.Gly1175Ser and p.Thr1298Ile have increased fibril variability, while p.Pro1444His has a slight increase in diameter. B) Bone tissues from two C-propeptide probands were examined by TEM or scanning electron microscopy (SEM). In TEM of proband bone samples, the collagen fibrils have irregular borders and a wide distribution of fibril diameters, in contrast to proband dermal collagen fibrils. SEM of α1(I) p.Pro1444His bone tissue shows individual fibrils of highly variable sizes.

in helical regions both lead to overmodification of the collagen chains. Although mature collagen helices in C-propeptide probands have a normal primary structure, mislocalization of collagen to the ER lumen and defective cleavage of the C-propeptide contribute to the mechanism of OI pathology. Further investigations in osteoblasts and bone tissue will be useful to show the full effects of the C-propeptide mutations.

Authorship statement

Aileen M. Barnes: Investigation, Formal analysis, Validation, Visualization, Writing-original draft. Aarthi Ashok: Investigation, Writing-original draft. Elena N. Makareeva: Investigation, Formal analysis. Marina Brusel: Investigation, Formal analysis. Wayne A. Cabral: Investigation. MaryAnn Weis: Investigation. Catherine Moali: Writing-Review & Editing. Emmanuel Bettler: Software, Investigation. David R. Eyre: Supervision. John P. Cassella: Investigation. Sergey Leikin: Supervision. David J. S. Hulmes: Conceptualization, Supervision, Writing- Review and Editing. Efrat Kessler: Methodology, Conceptualization, Supervision, Writing – Review and Editing. Joan C. Marini: Conceptualization, Resources, Supervision, Project Administration, Writing – original draft, Writing- Review & Editing.

Transparency document

The Transparency document associated with this article can be found, in online version.

Acknowledgements

We would like to acknowledge the families' contribution to OI research. The confocal microscopy was conducted in the NICHD Microscopy and Imaging Core. We thank Dr. James Pace (Dr. Peter Byers laboratory, University of Washington) for sharing the P6 cell line and Sarah A. Milgrom, M.D., (NICHD/NIH) for contribution to early studies on P5 and family.

Funding: This work was supported by NICHD Intramural Funding [J.C.M. and S.L]; the Israel Science Foundation [contract grant number 1360/07 (to E.K.)]; NIAMS/NIH [grants AR037318 and AR036794 (to D.R.E.)]; and the European Commission [project grant number NMP2-CT-2003-504017 (to D.J.S.H.)].

Disclosure statement: The authors declare no conflicts of interest.

Appendix A. Supplementary data

Supplementary data to this article can be found online at https://doi.org/10.1016/j.dummy.2019.01.002.

References

[1] D.O. Sillence, A. Senn, D.M. Danks, Genetic heterogeneity in osteogenesis imperfecta, J. Med. Genet. 16 (1979) 101–116.
[2] Marini, J. C. (2004) Osteogenesis imperfecta. In Nelson Textbook of Pediatrics (Behrman, R. E., Kliegman, R. M. and Jensen, H. B., eds.). pp. 2336–2338, W.B. Saunders, Philadelphia.
[3] J.F. Lees, M. Tasab, N.J. Bulleid, Identification of the molecular recognition sequence which determines the type-specific assembly of procollagen, EMBO J. 16 (1997) 908–916.
[4] U. Sharma, L. Carrique, S. Vadon-Le Goff, N. Mariano, R.N. Georges, F. Delolme, P. Koivunen, J. Myllyharju, C. Moali, N. Aghajari, D.J.S. Hulmes, Structural basis of homo- and heterotrimerization of collagen I, Nat. Commun. 8 (2017) 14671.
[5] A.S. DiChiara, R.C. Li, P.H. Suen, A.S. Hosseini, R.J. Taylor, A.F. Weickhardt, D. Malhotra, D.R. McCaslin, M.D. Shoulders, A cysteine-based molecular code informs collagen C-propeptide assembly, Nat. Commun. 9 (2018) 4206.
[6] H.P. Bachinger, P. Bruckner, R. Timpl, D.J. Prockop, J. Engel, Folding mechanism of the triple helix in type-III collagen and type-III pN-collagen. Role of disulfide bridges and peptide bond isomerization, Eur. J. Biochem. 106 (1980) 619–632.
[7] Kessler, E. (2013) Procollagen C-endopeptidase. In Handbook of Proteolytic Enzymes (GS, R. N. a. S., ed.). pp. 916–932, Academic Press, Oxford.
[8] E. Kessler, K. Takahara, L. Biniaminov, M. Brusel, D.S. Greenspan, Bone morphogenetic protein-1: the type I procollagen C-proteinase, Science. 271 (1996) 360–362.
[9] S. Vadon-Le Goff, D.J.S. Hulmes, C. Moali, BMP-1/tolloid-like proteinases synchronize matrix assembly with growth factor activation to promote morphogenesis and tissue remodeling, Matrix Biol. 44-46 (2015) 14–23.
[10] D.J.S. Hulmes, A.P. Mould, E. Kessler, The CUB domains of procollagen C-proteinase enhancer control collagen assembly solely by their effect on procollagen C-proteinase/bone morphogenetic protein-1, Matrix Biol. 16 (1997) 41–45.
[11] E. Kessler, R. Adar, Type I procollagen C-proteinase from mouse fibroblasts. Purification and demonstration of a 55-kDa enhancer glycoprotein, Eur. J. Biochem. 186 (1989) 115–121.
[12] C. Moali, B. Font, F. Ruggiero, D. Eichenberger, P. Rousselle, V. Francois, A. Oldberg, L. Bruckner-Tuderman, D.J.S. Hulmes, Substrate-specific modulation of a multisubstrate proteinase. C-terminal processing of fibrillar procollagens is the only BMP-1-dependent activity to be enhanced by PCPE-1, J. Biol. Chem. 280 (2005) 24188–24194.
[13] S. Symoens, D.J.S. Hulmes, J.M. Bourhis, P.J. Coucke, A. De Paepe, F. Malfait, Type I procollagen C-propeptide defects: study of genotype-phenotype correlation and predictive role of crystal structure, Hum. Mutat. 35 (2014) 1330–1341.
[14] J.M. Bourhis, N. Mariano, Y. Zhao, K. Harlos, J.Y. Exposito, E.Y. Jones, C. Moali, N. Aghajari, D.J.S. Hulmes, Structural basis of fibrillar collagen trimerization and related genetic disorders, Nat. Struct. Mol. Biol. 19 (2012) 1031–1036.
[15] P.G. Robey, J.D. Termine, Human bone cells in vitro, Calcif. Tissue Int. 37 (1985) 453–460.
[16] E. Krieger, G. Vriend, YASARA view - molecular graphics for all devices - from smartphones to workstations, Bioinformatics. 30 (2014) 2981–2982.
[17] E.F. Pettersen, T.D. Goddard, C.C. Huang, G.S. Couch, D.M. Greenblatt, E.C. Meng, T.E. Ferrin, UCSF chimera–a visualization system for exploratory research and analysis, J. Comput. Chem. 25 (2004) 1605–1612.
[18] J. Bonadio, P.H. Byers, Subtle structural alterations in the chains of type I procollagen produce osteogenesis imperfecta type II, Nature. 316 (1985) 363–366.
[19] E. Makareeva, E.L. Mertz, N.V. Kuznetsova, M.B. Sutter, A.M. DeRidder, W.A. Cabral, A.M. Barnes, D.J. McBride, J.C. Marini, S. Leikin, Structural heterogeneity of type I collagen triple helix and its role in osteogenesis imperfecta, J. Biol. Chem. 283 (2008) 4787–4798.
[20] A.M. Barnes, W. Chang, R. Morello, W.A. Cabral, M. Weis, D.R. Eyre, S. Leikin, E. Makareeva, N. Kuznetsova, T.E. Uveges, A. Ashok, A.W. Flor, J.J. Mulvihill, P.L. Wilson, U.T. Sundaram, B. Lee, J.C. Marini, Deficiency of cartilage-associated protein in recessive lethal osteogenesis imperfecta, N. Engl. J. Med. 355 (2006) 2757–2764.
[21] A.M. Barnes, W.A. Cabral, M. Weis, E. Makareeva, E.L. Mertz, S. Leikin, D. Eyre, C. Trujillo, J.C. Marini, Absence of FKBP10 in recessive type XI osteogenesis imperfecta leads to diminished collagen cross-linking and reduced collagen deposition in extracellular matrix, Hum. Mutat. 33 (2012) 1589–1598.
[22] A.C. Nicholls, J. Oliver, D.V. Renouf, D.A. Heath, F.M. Pope, The molecular defect in a family with mild atypical osteogenesis imperfecta and extreme joint hypermobility: exon skipping caused by an 11-bp deletion from an intron in one COL1A2 allele, Hum. Genet. 88 (1992) 627–633.
[23] J.F. Bateman, S.B. Golub, Deposition and selective degradation of structurally-abnormal type I collagen in a collagen matrix produced by osteogenesis imperfecta fibroblasts in vitro, Matrix Biol. 14 (1994) 251–262.
[24] L.W. Fisher, J.T. Stubbs 3rd, M.F. Young, Antisera and cDNA probes to human and certain animal model bone matrix noncollagenous proteins, Acta Orthop. Scand. Suppl. 266 (1995) 61–65.
[25] K. Lindahl, A.M. Barnes, N. Fratzl-Zelman, M.P. Whyte, T.E. Hefferan, E. Makareeva, M. Brusel, M.J. Yaszemski, C.J. Rubin, A. Kindmark, P. Roschger, K. Klaushofer, W.H. McAlister, S. Mumm, S. Leikin, E. Kessler, A.L. Boskey, O. Ljunggren, J.C. Marini, COL1 C-propeptide cleavage site mutations cause high bone mass osteogenesis imperfecta, Hum. Mutat. 32 (2011) 598–609.
[26] E. Kessler, R. Adar, B. Goldberg, R. Niece, Partial purification and characterization of a procollagen C-proteinase from the culture medium of mouse fibroblasts, Coll. Relat. Res. 6 (1986) 249–266.
[27] W.A. Cabral, E. Makareeva, A. Colige, A.D. Letocha, J.M. Ty, H.N. Yeowell, G. Pals, S. Leikin, J.C. Marini, Mutations near amino end of alpha1(I) collagen cause combined osteogenesis imperfecta/Ehlers-Danlos syndrome by interference with N-propeptide processing, J. Biol. Chem. 280 (2005) 19259–19269.
[28] J.P. Cassella, R. Pereira, J.S. Khillan, D.J. Prockop, N. Garrington, S.Y. Ali, An ultrastructural, microanalytical, and spectroscopic study of bone from a transgenic mouse with a COL1A1 pro-alpha-1 mutation, Bone. 15 (1994) 611–619.
[29] D.L. Bodian, T.F. Chan, A. Poon, U. Schwarze, K. Yang, P.H. Byers, P.Y. Kwok, T.E. Klein, Mutation and polymorphism spectrum in osteogenesis imperfecta type II: implications for genotype-phenotype relationships, Hum. Mol. Genet. 18 (2009) 463–471.
[30] R. Pollitt, R. McMahon, J. Nunn, R. Bamford, A. Afifi, N. Bishop, A. Dalton, Mutation analysis of COL1A1 and COL1A2 in patients diagnosed with osteogenesis imperfecta type I-IV, Hum. Mutat. 27 (2006) 716.
[31] S.M. Pyott, M.G. Pepin, U. Schwarze, K. Yang, G. Smith, P.H. Byers, Recurrence of perinatal lethal osteogenesis imperfecta in sibships: parsing the risk between parental mosaicism for dominant mutations and autosomal recessive inheritance, Genet. Med. 13 (2011) 125–130.
[32] H. Zhang, H. Yue, C. Wang, W. Hu, J. Gu, J. He, W. Fu, Y. Hu, M. Li, Z. Zhang, Clinical characteristics and the identification of novel mutations of COL1A1 and COL1A2 in 61 Chinese patients with osteogenesis imperfecta, Mol. Med. Rep. 14 (2016) 4918–4926.
[33] J.M. Pace, D. Chitayat, M. Atkinson, W.R. Wilcox, U. Schwarze, P.H. Byers, A single amino acid substitution (D1441Y) in the carboxyl-terminal propeptide of the proalpha1(I) chain of type I collagen results in a lethal variant of osteogenesis imperfecta with features of dense bone diseases, J. Med. Genet. 39 (2002) 23–29.

[34] D. Pulido, U. Sharma, S. Vadon-Le Goff, S.A. Hussain, S. Cordes, N. Mariano, E. Bettler, C. Moali, N. Aghajari, E. Hohenester, D.J.S. Hulmes, Structural basis for the acceleration of procollagen processing by procollagen C-proteinase enhancer-1, Structure. 26 e1383 (2018) 1384–1392.
[35] S.D. Chessler, G.A. Wallis, P.H. Byers, Mutations in the carboxyl-terminal propeptide of the pro alpha 1(I) chain of type I collagen result in defective chain association and produce lethal osteogenesis imperfecta, J. Biol. Chem. 268 (1993) 18218–18225.
[36] J.M. Pace, C.D. Kuslich, M.C. Willing, P.H. Byers, Disruption of one intra-chain disulphide bond in the carboxyl-terminal propeptide of the proalpha1(I) chain of type I procollagen permits slow assembly and secretion of overmodified, but stable procollagen trimers and results in mild osteogenesis imperfecta, J. Med. Genet. 38 (2001) 443–449.
[37] K. Beck, B.A. Boswell, C.C. Ridgway, H.P. Bachinger, Triple helix formation of procollagen type I can occur at the rough endoplasmic reticulum membrane, J. Biol. Chem. 271 (1996) 21566–21573.
[38] S.D. Chessler, P.H. Byers, BiP binds type I procollagen pro alpha chains with mutations in the carboxyl-terminal propeptide synthesized by cells from patients with osteogenesis imperfecta, J. Biol. Chem. 268 (1993) 18226–18233.
[39] J.E. Oliver, E.M. Thompson, F.M. Pope, A.C. Nicholls, Mutation in the carboxy-terminal propeptide of the pro alpha 1(I) chain of type I collagen in a child with severe osteogenesis imperfecta (OI type III): possible implications for protein folding, Hum. Mutat. 7 (1996) 318–326.
[40] S. Ricard-Blum, S. Bernocco, B. Font, C. Moali, D. Eichenberger, J. Farjanel, E.R. Burchardt, M. van der Rest, E. Kessler, D.J.S. Hulmes, Interaction properties of the procollagen C-proteinase enhancer protein shed light on the mechanism of stimulation of BMP-1, J. Biol. Chem. 277 (2002) 33864–33869.
[41] R.G. Phelps, A. Martinez-Hernandez, B.D. Goldberg, Ultrastructural immunocytochemical localization of type I procollagen in cultured human fibroblasts, Coll. Relat. Res. 5 (1985) 405–414.
[42] Y. Ishikawa, S. Ito, K. Nagata, L.Y. Sakai, H.P. Bachinger, Intracellular mechanisms of molecular recognition and sorting for transport of large extracellular matrix molecules, Proc. Natl. Acad. Sci. U. S. A. 113 (2016) E6036–E6044.
[43] V. Martinez-Glez, M. Valencia, J.A. Caparros-Martin, M. Aglan, S. Temtamy, J. Tenorio, V. Pulido, U. Lindert, M. Rohrbach, D. Eyre, C. Giunta, P. Lapunzina, V.L. Ruiz-Perez, Identification of a mutation causing deficient BMP1/mTLD proteolytic activity in autosomal recessive osteogenesis imperfecta, Hum. Mutat. 33 (2012) 343–350.
[44] F. Malfait, S. Symoens, N. Goemans, Y. Gyftodimou, E. Holmberg, V. Lopez-Gonzalez, G. Mortier, S. Nampoothiri, M.B. Petersen, A. De Paepe, Helical mutations in type I collagen that affect the processing of the amino-propeptide result in an osteogenesis imperfecta/Ehlers-Danlos syndrome overlap syndrome, Orphanet J. Rare Dis. 8 (2013) 78.
[45] J.M. Davidson, L.S. McEneany, P. Bornstein, Intermediates in the conversion of procollagen to collagen. Evidence for stepwise limited proteolysis of the COOH-terminal peptide extensions, Eur. J. Biochem. 81 (1977) 349–355.
[46] N.P. Morris, L.I. Fessler, J.H. Fessler, Procollagen propeptide release by procollagen peptidases and bacterial collagenase, J. Biol. Chem. 254 (1979) 11024–11032.
[47] W.N. Pappano, B.M. Steiglitz, I.C. Scott, D.R. Keene, D.S. Greenspan, Use of Bmp1/Tll1 doubly homozygous null mice and proteomics to identify and validate in vivo substrates of bone morphogenetic protein 1/tolloid-like metalloproteinases, Mol. Cell. Biol. 23 (2003) 4428–4438.
[48] M. Mizuno, R. Fujisawa, Y. Kuboki, The effect of carboxyl-terminal propeptide of type I collagen (c-propeptide) on collagen synthesis of preosteoblasts and osteoblasts, Calcif. Tissue Int. 67 (2000) 391–399.
[49] M. Mizuno, R. Fujisawa, Y. Kuboki, Carboxyl-terminal propeptide of type I collagen (c-propeptide) modulates the action of TGF-beta on MC3T3-E1 osteoblastic cells, FEBS Lett. 479 (2000) 123–126.
[50] M. Mizuno, T. Kitafima, M. Tomita, Y. Kuboki, The osteoblastic MC3T3-E1 cells synthesized C-terminal propeptide of type I collagen, which promoted cell-attachment of osteoblasts, Biochim. Biophys. Acta 1310 (1996) 97–102.
[51] S.A. Weston, D.J.S. Hulmes, A.P. Mould, R.B. Watson, M.J. Humphries, Identification of integrin alpha 2 beta 1 as cell surface receptor for the carboxyl-terminal propeptide of type I procollagen, J. Biol. Chem. 269 (1994) 20982–20986.
[52] C. Bantsimba-Malanda, J. Cottet, P. Netter, D. Dumas, D. Mainard, J. Magdalou, J.B. Vincourt, Chondrocalcin is internalized by chondrocytes and triggers cartilage destruction via an interleukin-1beta-dependent pathway, Matrix Biol. 32 (2013) 443–451.
[53] K. Nakata, S. Miyamoto, S. Bernier, M. Tanaka, A. Utani, P. Krebsbach, C. Rhodes, Y. Yamada, The c-propeptide of type II procollagen binds to the enhancer region of the type II procollagen gene and regulates its transcription, Ann. N. Y. Acad. Sci. 785 (1996) 307–308.
[54] C.H. Wu, C.M. Walton, G.Y. Wu, Propeptide-mediated regulation of procollagen synthesis in IMR-90 human lung fibroblast cell cultures. Evidence for transcriptional control, J. Biol. Chem. 266 (1991) 2983–2987.
[55] R.E. Wuthier, G.F. Lipscomb, Matrix vesicles: structure, composition, formation and function in calcification, Front. Biosci. 16 (2011) 2812–2902.
[56] A.A. Choglay, I.F. Purdom, D.J.S. Hulmes, Procollagen binding to sphingomyelin, J. Biol. Chem. 268 (1993) 6107–6114.